



OPEN Remotely extinguishing flames through transient acoustic streaming using time reversal focusing of sound

Jay M. Cliftmann & Brian E. Anderson

Acoustic waves are a possible reusable method to extinguish flames. Previous studies have placed the sound source near the flame or have used standing waves to reach large enough acoustic amplitudes to extinguish it. In this study, a new method is explored: using time reversal in a room to focus transient acoustic waves to the flame to extinguish it. The peak acoustic overpressure level needed to extinguish a candle flame in the middle of the room is 191 dB_{peak} re 20 μPa when using a frequency range of 300 to 15000 Hz. The sound level at other locations of the room during the focusing was 130 dB. The required peak level is lower when using a less stable flame, or when the flame is near a room boundary. The momentary focus of high-amplitude sound waves subsequently causes acoustic streaming or a flow of air at the flame location that extinguishes the flame. By analyzing high-speed video, it is shown that acoustic streaming extinguishes the flame when using this method, not the acoustic particle displacement. It is also shown that the streaming does not occur when the flame is not present.

Keywords Acoustics, Time reversal, Acoustic streaming, Nonlinear acoustics, Flame extinction, High-speed imaging

Using acoustic waves to extinguish flames has been studied for its novelty and potential. Acoustic extinguishing of a flame has been studied because if it became practical, it would be environmentally friendly, reusable, and would not cause damage to equipment^{1–5}. It also has the potential to be safe around people. However, using sound to extinguish flames has shortcomings, such as the proximity of the sound source to the flame or the size of flames that can be extinguished^{5,6}. These shortcomings stem from the mechanisms that extinguish the flame.

Recent literature suggests two main mechanisms for how the acoustic wave extinguishes small flames. The first is that the oscillating acoustic particle velocity caused by the passing pressure wave contributes to the extinction by displacing the flame back and forth (the oscillating partial vacuum in the rarefactions of the sound wave does not affect the flame significantly)^{6–9}. The second mechanism is a net, unidirectional flow of air from the sound source that unidirectionally deflects the flame, also contributing to extinction¹⁰. Though not reported, net flow can be seen as the unidirectional deflection of the flame to one side in the images of much of the existing literature^{3–6,8–12}. This net flow should not be confused with the “speaker-induced wind” noted by Xiong et al. which is an oscillatory, particle displacement that is larger than predicted by the sound pressure level measured at the location of the flame. This “speaker-induced wind” discrepancy is likely caused by modeling the acoustic source as a plane wave rather than a monopole.

The net flow and vortices (or vortex rings) produced by a sound source are considered acoustic streaming^{13,14}. Acoustic streaming is a nonlinear effect caused by both dissipation and by the sound wave interacting with a boundary^{14,15}. When streaming occurs, the airflow is often rotational^{14,16}. To achieve streaming, one often uses a long-duration, finite-amplitude, steady-state sound wave using continuous-wave excitation^{14–16}. However, short-duration, aperiodic sounds are known to also cause streaming^{17,18}. Streaming has been studied heavily for biomedical applications as well as for fluid mixing and boundary cooling¹⁵.

Both a net flow of air and vortex rings are seen when high-amplitude and low-frequency sound waves pass through holes^{13,14}. This is considered acoustic streaming. Both high-amplitude and low-frequency waves are used for many of the flame extinction studies cited here, and some of them have hole-like apertures that the acoustic wave exits. For instance, in the context of the design of loudspeaker ports, acoustic streaming from a loudspeaker operating at high amplitudes has been shown to create vortex rings moving away from the port^{19–23}.

Acoustics Research Group, Department of Physics and Astronomy, Brigham Young University, Provo 84602, USA.
✉ email: bea@byu.edu

Furthermore, vortex rings are effective at extinguishing flames at longer distances, perhaps explaining why some acoustic extinguishing devices are effective at large distances²⁴. What this means for many of the past studies is that both oscillatory particle velocity and acoustic streaming contributed to extinction.

Anyone can see acoustic streaming and can even extinguish small flames with their smartphone speakers using any “blower”-type app (search for “blower” on the app store). The app plays loud sounds from the smartphone, and, because the holes for the sound to get out are so small, there is a net flow from the device that can extinguish small flames. The effect of the net flow and vortex rings from a sound source on extinguishing amplitudes or distances is not well understood and should be studied further. Despite not being well understood, some have exploited it in the design of their sound source by creating a small-diameter, loudspeaker-like port with sharp edges that can blow out flames from longer distances^{2,4}. The pipes or waveguides some researchers have attached to their loudspeakers can cause acoustic streaming. Loudspeakers themselves (not the waveguides or ports) may cause a net flow of air aiding in the extinction of small flames.

Of the two mechanisms (oscillating acoustic particle velocity and acoustic streaming), most of the studies have sought to maximize the oscillating air particle velocity at the location of the flame. Low-frequency sound waves have a larger particle velocity, so many studies have shown that lower-frequency waves are better for putting out flames^{1–3,5–7,10–12,25–30}. Beyond using low frequencies, recent research can be placed into two main categories based on how they maximize acoustic particle velocity. The first group places the flames very close to the sound source, and the second group uses standing waves in rooms or pipes to extinguish a flame.

In the first group, the flame has been placed near the sound source^{1–11,26,27,29–31}. Researchers either placed the flame right next to the loudspeaker^{1,3,6,8,9,30} or they attached a pipe (waveguide) to the loudspeaker and placed the flame near the end of that^{2,4,7,8,10,11,26,27,29,31,32}. They attach a waveguide to channel the sound and to avoid burning the loudspeaker. The flame was placed as little as 3 cm from the loudspeaker or waveguide to achieve large enough particle velocities for extinguishing³¹. Wilk-Jakubowski *et al.*^{26,27} and Taspinar *et al.*⁴ were able to extinguish flames at much larger distances. The first used the resonance of the attached waveguide at 17 Hz to generate a large enough amplitude to extinguish a flame 1.2 m away, and the second used a loudspeaker port excited by four drivers to generate a large enough amplitude to extinguish a flame at 1.9 m away from the port at about 15 Hz. The large distances from the source were possible because they used lower frequencies and because their devices likely exploited the acoustic streaming generated at the port of low-frequency sources^{4,10,19–24}. Unfortunately, all of the studies in the first group did their experiments in rooms and thus standing waves or reflections from walls may have impacted their findings. More work needs to be done to separate the impacts of placing flames near the sound source versus room effects such as standing waves or reflections from walls.

For the second smaller group, the flame is extinguished by exciting a standing wave in a room or pipe with the flame inside it^{11,25}. By using standing waves, the researchers might eliminate the acoustic streaming mechanism, putting out the flames using only acoustic oscillations. However, this would need to be verified because streaming can exist in standing waves¹⁴. The main effort for using standing waves to extinguish flames was by unnamed researchers working for DARPA (the United States Defense Advanced Research Projects Agency)¹¹. They used standing waves to extinguish a flame 2 m from the source at a frequency that excited a room mode. At neighboring frequencies above and below the resonance, the flame was not extinguished. In addition, they found that they could extinguish a flame near a wall of the room where there is theoretically zero acoustic particle velocity in a standing wave. They offered no explanation for the flame’s extinction in this case. Further work needs to be done to understand this phenomenon.

In this paper, we present a third method of extinguishing flames using sound waves: high-amplitude focusing of sound from a distance. This eliminates the effect of acoustic streaming near the sound sources because the sound sources are far away. Also, the focusing happens quickly enough that standing waves are not set up. Time Reversal (TR) is a signal processing technique^{33–36} that has been used, among other things, to focus high amplitude sound to a selected location for a brief moment in time^{37–39}. TR works better in a reverberant environment because it causes all of the reflections to constructively add at the focal location. The ability of TR to create high amplitudes has been studied extensively for biomedical treatments^{40–44}, for non-contact excitation^{45–47}, for nondestructive testing^{36,46–51}, and in rooms^{37,38,52–54}. Patchett *et al.*³⁷ used TR of audible sound in rooms to reach peak focal amplitudes of 200.6 dB. Patchett *et al.* also reported wave steepening in TR focusing in rooms, a nonlinear effect^{37,38,53}. TR has been shown to cause acoustic streaming at sufficiently high amplitudes using steady-state ultrasound^{55–57}. Similar to Patchett *et al.*³⁷, we use TR in a reverberation chamber to generate acoustic waves with amplitudes high enough to extinguish a small flame. We also show that high-amplitude, transient TR focusing of audible frequencies in air can cause acoustic streaming, and it is the streaming that extinguishes flames while using this method.

We report here on the extinguishing of a candle flame far from multiple sources. By using TR at frequencies of 300 to 15000 Hz, we can achieve brief localized pressures of amplitude sufficient to extinguish a candle flame. We also show evidence suggesting that the mechanism for extinction when using TR is acoustic streaming.

Methods

Time reversal acoustics

TR can be done in multiple ways using any type of wave. Here we use multichannel TR using audible acoustic waves in rooms³⁵. Multichannel indicates that we are using more than one loudspeaker simultaneously. To start the TR process used here, one places a microphone at the desired focal location in the room. One by one, each sound source broadcasts a chirp signal into the room while the microphone records a chirp response. Each of these separately-recorded chirp responses is then processed with the broadcast chirp signal to retrieve the impulse response (IR) from each source to the microphone location. This process is essentially a deconvolution operation and is done digitally using a cross-correlation^{58,59}. This process yields a high quality IR with a higher signal to noise ratio than if a pulse was instead emitted to obtain the IR. Each IR contains the timing of each

arrival of the broadcast wave at the microphone. The majority of arrivals reflect off of multiple walls before reaching the microphone. Each IR is then digitally reversed in time, hence the name time reversal.

To better understand how the TR process works, it will be helpful to consider only one source. After the IR from this source is reversed in time, the time-reversed impulse response (TRIR) will then be broadcast from that same source. The timing of each emission from the source will be reversed relative to their original arrival times at the microphone. This means that the part of the signal played first will correspond to the path that took the longest time to travel between the source and the microphone, the second part of the signal played will correspond to the second longest path, and so on. After all of the TRIR is played, some portion of each emission of the TRIR will arrive at the microphone at the same time, constructively adding. The constructive interference of the many arrivals of waves at the microphone location is a result of reversing the timing of the reflections in the IR. Some energy travels these same reflection paths, and this reversed timing ensures that the energy that traverses these many paths arrives in phase at the microphone. Late reflections in the IR are broadcast first and have time to travel their paths, followed by early reflections that need less time to travel to the microphone, and finally the direct sound emission. Some amount of energy arrives coherently from all of these paths, creating the TR focusing. In a sufficiently reverberant room, this causes a spherical converging focus at the microphone from only one source⁶⁰.

In this study, we will be using eight sources as shown in Fig. 1. When we use all eight sources, each source can individually focus to the microphone. By time aligning the broadcasts from all sources, the foci from each different source constructively add, resulting in a spherical focus about eight times or 18 dB larger in amplitude than the focus of a single source.

The TR process is depicted in Fig. 2 where (a) is the chirp signal, (b) is the recorded chirp response from one loudspeaker, (c) is the TRIR for one loudspeaker, and (d) is the recorded focal signal while broadcasting all eight TRIRs simultaneously. The chirp signal is a 6-second linear sine sweep from 300 Hz to 15000 Hz with a cosine-tapered window. The cosine-tapered window is used to smooth out discontinuities when starting and stopping the chirp signal⁶¹. This chirp signal dictates the range of frequencies used during the focusing.

What also determines the spectral content present in the focal signal is the frequency response of the room. A reverberation chamber is used with dimensions of $5.69 \times 4.32 \times 2.49$ m (61 cubic meters), a reverberation time of 4.16 s, and a Schroeder frequency of 522 Hz (the boundary between the modal region and the diffuse field region of a room). It is shown schematically in Fig. 1. The room also has plexiglass panels erratically hung from the ceiling which introduce random scattering of waves in the room but also increase absorption at higher frequencies. Because the room has higher absorption at higher frequencies, the low-frequency energy (about 300 Hz to 2000 Hz) dominates the focus. The spectrum of the focus signal is shown in Fig. 3. Of note in the spectrum is the negligible amount of energy above 5 kHz in the focus.

High-amplitude acoustic waves are needed to extinguish flames. Prior research explored techniques to increase the amplitude of TR focusing. We employ several of these techniques in this study. First, we place the loudspeakers facing away from the focal location as shown schematically in Fig. 1⁵⁸. Second, we place the loudspeakers very close to the walls to increase the radiation efficiency of the loudspeaker⁵⁴. Third, we perform all of these experiments in a reverberation chamber as TR can use the extra reflections to increase the amplitude of the focus^{38,62,63}. Fourth, we digitally clip the TRIRs^{38,51}. As clipping decreases focal quality (temporally and spatially), this method was used as a last measure to increase amplitude. We clipped the ± 1 magnitude TRIR signal to a ± 0.1 threshold. After this, we re-normalized the signal to be ± 1 again.

We used custom LabVIEW software to generate the signals used in this process⁶⁴. These signals were output from the computer using two Spectrum M2i.6022-Exp cards before being amplified by two 4-channel Crown CT4150 amplifiers. These amplified signals were then sent to the sources, eight BMS 4590 coaxial compression drivers with horns. The acoustic waves were recorded using a PCB 112A23 microphone and a GRAS 12AX CCP power supply and digitized with a Spectrum M2i.4931-Exp card sampling at a frequency of 250 kHz with a bit rate of 16 bits. The software, cards, amplifiers, and microphone power supply are combined into the box labeled “Computer” in Fig. 1.

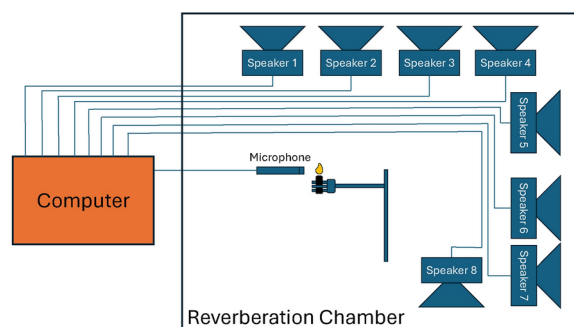


Figure 1. A visual schematic of our experimental setup. It shows eight horn drivers in a reverberation chamber. It also shows a microphone and a lit candle. The candle was not lit and the microphone was placed at the location of the flame to measure impulse responses from each horn driver. The microphone was then removed and the candle was lit before the focusing and extinguishing events. The box labeled computer contains the software, cards, amplifiers, and microphone power supply needed to perform the experiment.

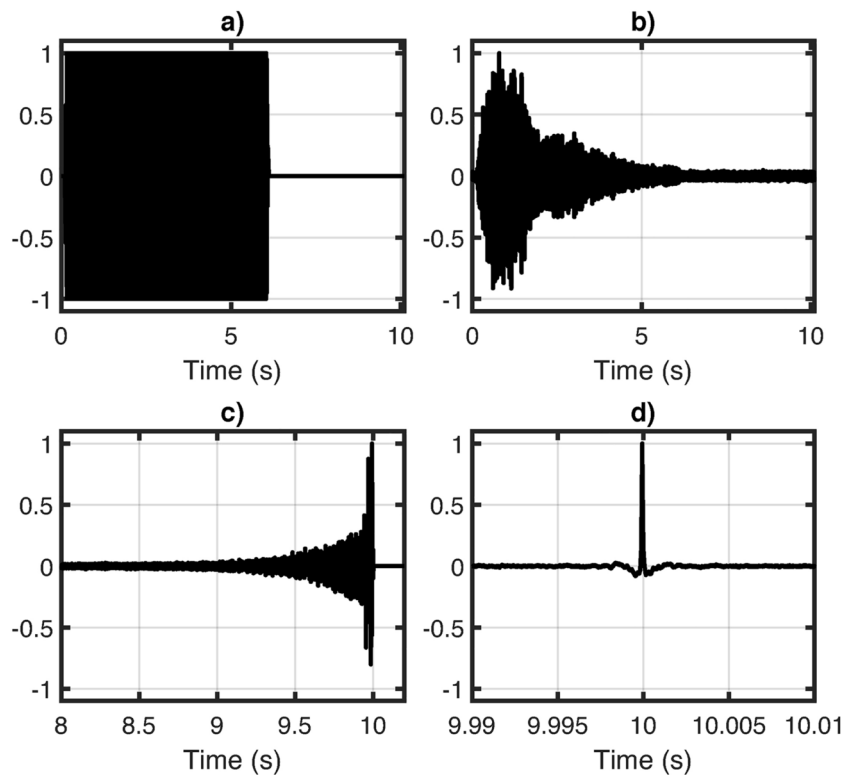


Figure 2. Normalized example signals used throughout the time-reversal process. (a) shows the chirp signal that is broadcast from each source. (b) shows the chirp response from one source after the broadcast. (c) shows the time-reversed impulse response for one source. (d) shows the focus signal after broadcasting from each source. Note the different time scales on each graph.

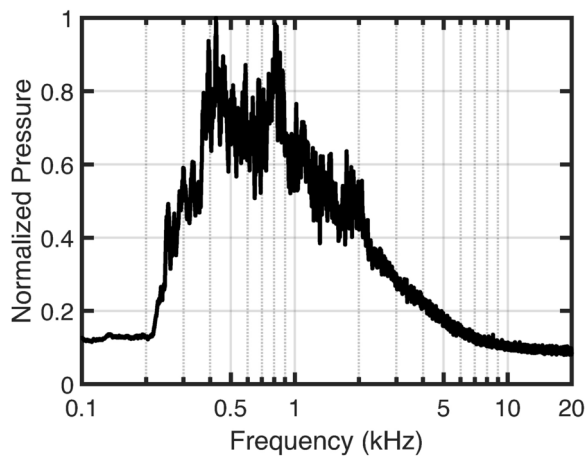


Figure 3. The normalized spectrum of the focus signal. Due to the higher absorption of higher frequencies in the room, there is more low-frequency energy present in the spectrum.

We also used an Applied Motion translational stage to move the microphone programmatically. By broadcasting the TRIRs and recording at different positions, we can get the pressure signal at many different points in space and, assuming repeatability, can reconstruct the pressure field experienced by the flame and the surrounding area both spatially and temporally.

Description of candle flames

A candle was used as the source of our flame. A thin, cylindrical, fast-burning candle was used to minimize reflections of sound off of the candle. The candle is shown schematically in Fig. 1. Different shapes of candles and different-sized flames affected the required peak sound pressure level needed to extinguish the flames,

so a thin, cylindrical candle was picked to eliminate the effect of the shape of the candle. Candle flames are laminar diffusion flames³². The average height of the candle flames in these experiments was about 2 cm. To eliminate acoustic boundary effects the candle was mounted high above the ground by a small lab clamp as shown schematically in Fig. 1. The candle, flame, and lab clamp can be seen later in Fig. 5.

The procedure for using TR to extinguish flames is as follows. A microphone was placed just above the unlit candle wick where the flame would be if the candle were lit. The individual IRs from each of the eight sources were obtained. All TRIRs were broadcast simultaneously and a focal signal was recorded from which loudness could be measured. Then the microphone was moved out of the way and the candle was lit. The TRIRs were then broadcast again to extinguish the flame. Once extinguished, the candle can be re-lit and re-extinguished multiple times using the same TRIRs.

The microphone (and thus the focus) was placed at the expected central location of the flame to measure the peak amplitudes needed for extinguishing. We also placed the focus above or to the side of the flame when tracking the flame in high-speed footage to better see the flame displacement due to acoustical particle displacement, acoustic streaming, and the resulting extinguishing. The focal location is not at the center of the flame for each high-speed video result shown here.

Video equipment and processing techniques

A Phantom V1610 high-speed camera was used to capture the extinction event. A frame rate of 20,000 fps was used and each video was exported and played at 30 fps as seen in the supplementary material.

To find the displacement of the flame, we tracked the position of the flame from the high-speed video. We took each frame of the video and noted each group of pixels that exceeded a brightness threshold. Then we calculate the centroid location of the group of bright pixels associated with the flame. Tracking the location of the centroid over time gives us time-dependent X and Y positions of the flame. This method of tracking the movement of the flame stops being effective at tracking flame displacement when the flame changes shape just before extinction.

Results

Extinction metric

To determine what acoustic focal amplitudes successfully extinguished the candle flame, we lit and attempted to extinguish the candle flame at least 8 out of 10 times. For those 10 measurements, we measured one set of IRs to focus to the first 5 lit candles, and then we measured a second set of IRs to focus to the second 5 lit candles. Changing the focal amplitude by 1 dB increments, the minimum peak sound pressure level at which the candle flame was extinguished 8 out of 10 times was 191 dB_{peak} re 20 μPa. For that focal amplitude, the spatially-averaged overall sound pressure level at other locations in the room was 130 dB_{rms} for 12 seconds. If a person is not at the location of the focus, the sound level they will experience is 12 seconds of 130 dB. This is technically acceptable within OSHA standards (the United States Occupational Safety and Health Administration), but people begin to experience pain at this loudness⁶⁵.

This threshold peak level, 191 dB_{peak}, is only valid for these specific candles placed far from walls where the focal location is at the position of the flame. If we change any of those three things, then the threshold level changes. First, the threshold level for extinguishing decreases for shorter or less stable flames, agreeing with the literature^{4,6,11}. Second, the closer the flame is to a wall or boundary, the lower the amplitudes needed to extinguish the same flame, possibly due to increased levels of streaming that occur near boundaries. Finally, the amplitude of the foci needed to extinguish a flame changes as the distance from the focal location to the flame varies until there is no extinction when the focus is far from the flame. We did not explore the latter relationship extensively in this study, but we can typically extinguish a flame within ±5 cm of the focus at 191 dB_{peak}.

Because the focused wave will only extinguish a flame near the focal location, it allows us to extinguish a single candle flame without extinguishing others around it. A real-time (not high-speed) video of this can be found in Supplementary Video S1. This provides an interesting educational demonstration of how TR-focused sound waves can be used to target a single location, in this case extinguishing one flame among many. It is similar to work done by others to demonstrate TR focusing^{66–68}.

Flame displacement and time of extinction

Snapshots at 1.5 and 0.75 ms time intervals of example candle flames being extinguished can be seen in Fig. 4 and in Fig. 5, respectively. The position of the spherical TR focus is shown with a white colored “x” on each image. The corresponding video can be found in Supplementary Videos S2 and S3. For these images, we have placed the focus above (Fig. 4) and to the side of (Fig. 5) the flame to better explore how the flame is extinguished.

Figure 6 parts (a) and (b) show the X and Y displacement of the flames’ centroids shown in Fig. 4 and Fig. 5, respectively. Also shown is the approximate predicted acoustic particle displacement obtained from microphone recordings. The process of getting the approximate predicted acoustic particle displacement is described in more detail in section 3.3. Each dataset (X, Y, and Predicted) is offset on the y-axis by 5 mm for visual clarity. A vertical yellow bar highlights the portion of time that the flame is displaced by the passing acoustic wave as predicted by the approximate acoustic particle displacement.

Before the arrival of the acoustic focal wave (the region to the left of the yellow highlight in Fig. 6), the position of the flame varies only slightly. When the acoustic focus converges (the portion of time highlighted yellow), the flame moves very quickly toward the focus and then back to its original position. This movement toward the focal location is mostly in the Y direction in Fig. 6a and mostly in the X direction in Fig. 6b because the focal locations were above and to the right, respectively, in those experiments. After the acoustic focus diverges and moves away from the flame, the centroids of both flames move slowly toward their respective focal locations, but now in one consistent direction. These are the portions of time in Fig. 6 after the yellow highlights. Finally,

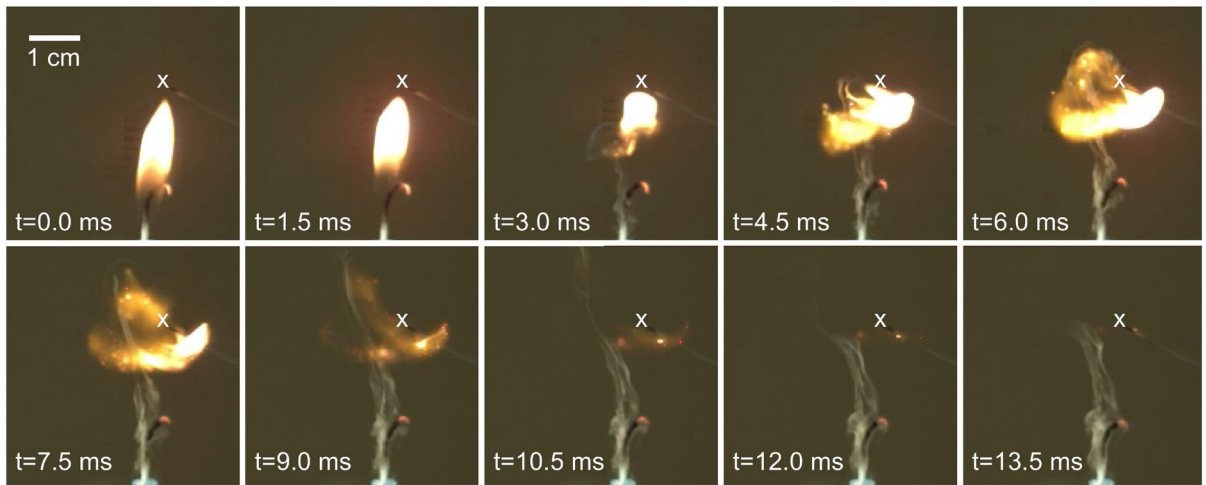


Figure 4. Ten video frames, 1.5 ms apart, of a flame as it is extinguished. The time is shown in the bottom left corner of each frame. The focal event occurs at the $t = 1.5$ ms frame. There is a white colored “x” overlaid at the position of the focus above the flame. Also shown is a 1 cm scale bar in the first frame. The corresponding video is found in Supplementary Video S2.

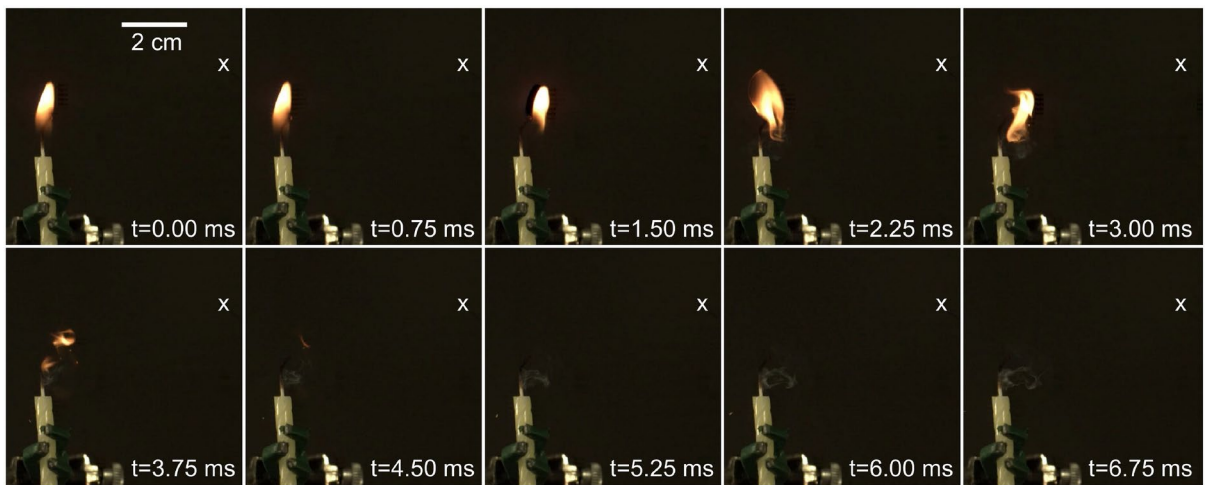


Figure 5. Ten video frames, 0.75 ms apart, of a flame as it is extinguished. The time is shown in the bottom right corner of each frame. The focal event occurs at the $t = 1.5$ ms frame. There is a white colored “x” overlaid at the position of the focus to the side of the flame. Also shown is a 2 cm scale bar in the first frame. The corresponding video is found in Supplementary Video S3.

when both flames are extinguished, the centroids move from one fragment of the original flame to another until no portions of the flame exceed the brightness threshold, and the flame is gone. In Fig. 6, this is visible when the movements of the centroids are erratic and then disappear. Figures 4 and 5 show the video frames of maximum acoustic particle displacement at $t = 1.5$ ms. The frames do not show the movement of the flame due to the acoustic particle displacement very well because the movement of the flame due to the acoustic wave happens within 0.5 ms. However, the brief, back-and-forth movement of the flames due to the acoustic focal event is visible in the corresponding videos in Supplementary Videos S2 and S3.

By putting the predicted acoustic particle displacement on the same time scale, we see that the flame experiences the acoustic particle displacement from the focused sound wave, but nothing in the acoustic data describes or predicts what happens after the yellow highlighted sections of Fig. 6 (because microphones do not detect static flows and, as we will find out is important, the flame was not present when the acoustic data used to predict the particle displacement was taken). The time alignment of the flame displacements from the video and the predicted acoustic displacements extracted from the microphone recordings will be discussed in the next section.

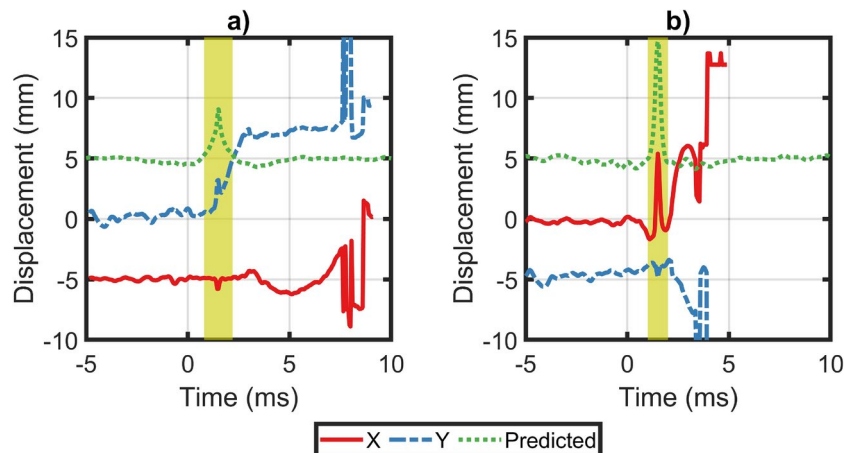


Figure 6. In both (a) and (b), the X (in red, solid) and Y (in blue, dashed) displacement of the flame's centroid shown versus time. Positive values in X denote a displacement to the right in the video frame and positive values in Y denote up in the video frame. The approximate predicted acoustic particle displacement at the location of the flame is also plotted (in green, dotted) and was numerically calculated from a similar acoustic pressure field. The datasets are offset by 5 mm on the vertical axis for visual clarity. The time range over which the acoustic wave focuses is highlighted in yellow and the focal events in both (a) and (b) occur at 1.5 ms. Graph (a) corresponds to Fig. 4 and graph (b) corresponds to Fig. 5. The time values on the horizontal axis correspond exactly to the time values on the frames of Figs. 4 and 5.

Acoustic displacement

Flame movement in most acoustic fields can be predicted well by acoustic particle displacement⁶. Before time-aligning, we first calculate the expected acoustic displacement from the spatial dependence of a measured pressure wave field of a high amplitude TR focus. By doing so, we can predict flame movement.

The acoustic particle displacement can be approximated using the well-known linear Euler's equation (momentum equation):

$$\rho \frac{\partial \vec{V}}{\partial t} = -\nabla P \quad (1)$$

where ρ is the static density of air, V is the acoustic particle velocity, ∇ is the gradient operator, and P is the acoustic pressure. If we know P at many spatial points in the acoustic field we can solve for the particle velocity, V , and from that the acoustic particle displacement.

We can only get approximate values for the displacement from this equation because the pressure waves are at high enough amplitudes to have significant non-linear effects^{37,38,52,53}. So, using a linear Euler's equation with these waves will only yield approximate values that can provide a qualitative understanding. Despite this, the approximate displacement values we get from the linear Euler's equation will allow us to time align the acoustic displacement with the flame displacement observed in the video, giving us insight into when the focal event occurred compared to the extinction of the flame.

We found the acoustic pressure field in both time and space throughout the focal region of a high-amplitude focus using the translation stage equipment discussed in the Methods. The pressure field consists of time signals recorded at 181 positions along a line that includes the focal position. The total length of the 1D scan of the pressure field is 1.8 m with 1 cm spacing. Numerically integrating the pressure twice in time and then taking the gradient at all individual time steps, or in this case just a numerical spatial derivative in 1D, gives us the estimated acoustic particle displacement at each point in space. Both the pressure and the acoustic particle displacements are shown as a function of position in Fig. 7 at the time of maximal focusing. Note the two vertical axes on the left and the right, one for pressure and one for displacement. The focal position is at 0.9 m. A negative displacement indicates a displacement in the negative X direction. The displacement in Fig. 7 has positive and negative peaks at a distance of ± 3 cm on either side of the focal position. The center of the focal position experiences a negligible amount of particle displacement throughout all time. Because the flame has some spatial extent, if the flame is centered at the focal position it will be slightly compressed but no translation motion will occur due directly to acoustic particle displacement.

We can see the estimated particle displacement and the translation motion of the flames as a function of time in Fig. 6. The flame is 1 cm away from the focal location in Fig. 4 and 5 cm away from the focal location in Fig. 5. Because the flame and the focal location are not collocated, we overlaid the predicted particle displacement for a particle that is 1 cm and 5 cm away from the focus onto Fig. 6a,b, respectively. The features highlighted in yellow of the tracked flame displacements match in shape to the features in the time signals of the estimated acoustic displacements, but they are smaller in amplitude than the measured flame displacements by 1 mm and

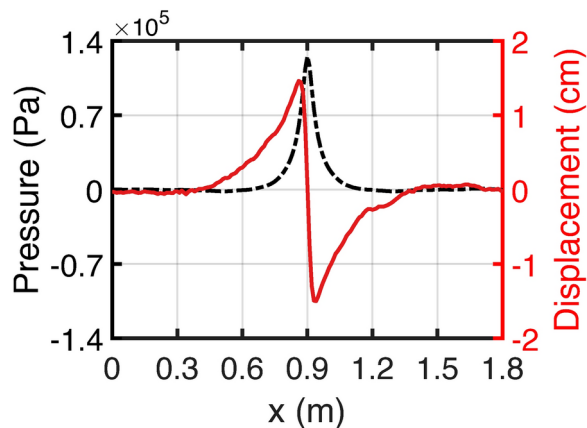


Figure 7. The spatial extent of the pressure and the acoustic particle displacement (obtained using the linear Euler's Equation) at peak focal time. The pressure, in dashed black, has axes on the left while the displacement, in solid red, has axes on the right. The focal position is at 0.9 m.

5 mm, respectively. Because the acoustic particle displacement and the flame displacement have similar shaped features, we can time align the flame displacement with the acoustic particle displacement using those features.

After time alignment, we can see that the flame is extinguished (has no more bright spots in the video frames) about 9 ms and 3 ms, respectively, after the focal event. Those delay times correspond to the focused acoustic waves having traveled about 3 m and 1 m, respectively, away from the flame by the time the flame extinguishes. Thus, the acoustic focal waves initialize the extinguishing event but do not directly cause the extinguishing of the flame.

Cause of extinction

The flame extinguishes when it is moved away from the fuel source (the candle's wax that evaporates off of the wick) for enough time to burn out, for the fuel source to cool, or a combination of those two effects. This is known as blow-off^{24,69,70}. This long movement away from the fuel source can be seen after the yellow highlight in Fig. 6. In this time region, the acoustic wave is no longer affecting the flame. This begs the question: What is pushing the flame away from the wick after the acoustic wave is gone?

To visualize the movement of air near the flame we placed a flat bundle of thin polyester fibers next to the flame. The video frames for 2 different videos are shown in Fig. 8. The top 5 frames, Fig. 8a, show the results of a focus without a flame present. The bottom 5 frames, Fig. 8b, show the results of a focus with a flame present. Both videos are aligned so that their foci occur simultaneously. In the first set of frames, the fibers are deflected a very small amount, however, when the flame is present during the focus in the second set of frames, the thread deflects much more. When the flame is present, the thread deflects to the left around the top of the flame while the flame deflects to the right. There is an apparent counter-clockwise rotational flow of air that causes these movements and causes the extinction of the flame. This rotational airflow after the acoustic event extinguishes the flame and is evidence of acoustic streaming.

Thus, the flame is extinguished by acoustic streaming, a non-oscillatory flow of air generated by nonlinear acoustic effects. We believe streaming is present because the translational and rotational motion of the flame and thread indicate a rotational flow of air that is typical of streaming. It is also acoustic streaming because the acoustic particle velocity (the fast back-and-forth movement of the flame) is much larger than the steady air velocity seen in the slower movement of the flame or thread after the acoustic event, which is also typical of airflow caused by streaming^{14,16}. Additionally, a mean flow of air after the focusing of the acoustic waves, can be observed in both Figs. 4 and 5, but the streaming is most prominent in Fig. 8b. The slow movement of the flame (and the air around the flame) after the yellow highlight in Fig. 6 is caused by the acoustic streaming. The acoustic wave initiates the streaming, but the streaming continues after the focal wave is gone and blows the flame out.

Why then is acoustic streaming happening in this case? Streaming typically occurs in high-amplitude and/or high-frequency waves near boundaries and in viscous fluids^{14,16}. While the frequencies used here are not considered very high and the air is not particularly viscous, the waves used are very high in amplitude and there is an acoustic boundary present in this situation. Comparing the motion of the thread in Fig. 8a,b shows that the thread moves very little when the flame is not originally present. The acoustic boundary in this situation appears to be the change in sound speed caused by the column of hot air above the flame, and this boundary may be initiating a preferred direction of flow for the streaming. Laminar flames have a laminar column of hot air flowing upward due to convection (also called the thermal plume of the flame)⁷¹. It can be seen in Schlieren images of any flame⁷¹. The column of hot air is not present when the candle is not lit, so the streaming does not happen. That is why the thread does not move much in Fig. 8a. Typically, TR would account for sound speed changes like the column of hot air in the IR, keeping the focus spherically symmetric. However, the IRs were collected when the candle was not lit so the column of hot air was not accounted for in the TRIRs used for

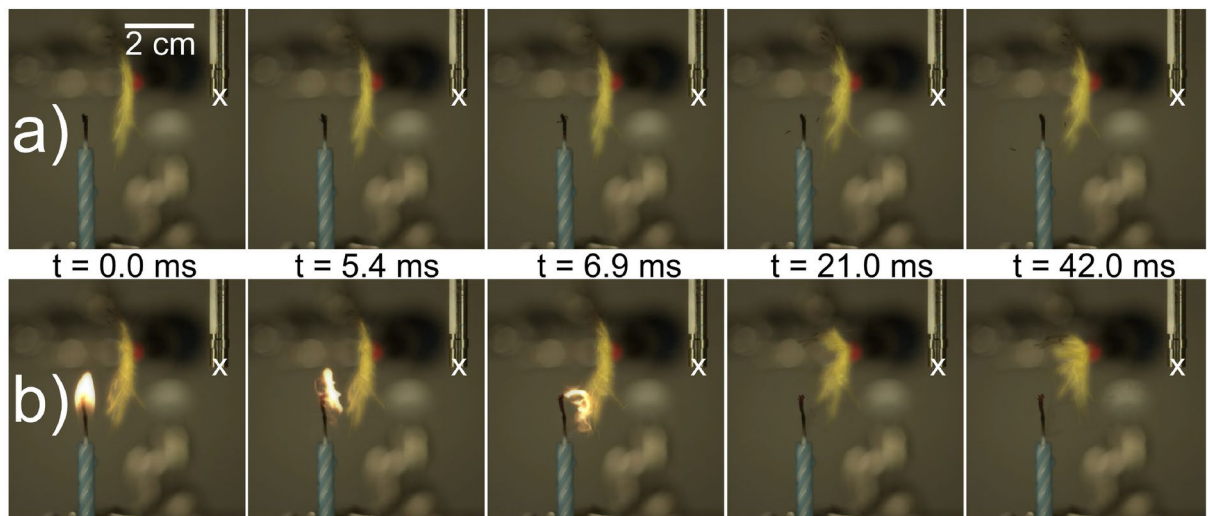


Figure 8. Two sets of video frames from 2 different videos. (a) consists of the top 5 video frames and is from the first video. (b) consists of the bottom 5 video frames and is from the second video. (a) contains no flame, but (b) shows a flame being extinguished. The videos are aligned in time with their focal events for visual comparison. There is a white colored “x” overlaid at the position of the focus. Also shown is a 2 cm scale bar in the first frame.

focusing. The hot column of air probably causes an asymmetry in the spherically converging wave increasing the likelihood of streaming and blowing out the flame.

Discussion and conclusion

This work demonstrates a new method to remotely extinguish flames using acoustic waves, namely Time Reversal (TR) focusing. In this study we have shown that TR focusing can be used to extinguish flames when the peak pressure at the flame is above $191 \text{ dB}_{\text{peak}}$ re $20 \mu\text{Pa}$ while the spatially-averaged overall sound pressure level at other locations of the room was $130 \text{ dB}_{\text{rms}}$. This peak amplitude threshold depends on flame height and proximity of the flame to walls or the focal location. The flame is extinguished as it is blown from the wick by acoustic streaming, rather than by acoustic displacement. The acoustic streaming is present well after the acoustic wave focuses due to both the high amplitudes present and the asymmetric column of hot air above the flame which changes the sound speed of portions of the focusing acoustic waves.

TR focusing of acoustic waves is a new method to extinguish flames using sound. TR excels in reverberant environments, such as inside buildings. Because it is a focused wave, it could be quiet enough to protect people’s hearing who are located away from the focal location, but loud enough at the flame to extinguish it. Further research could explore means to decrease amplitudes away from the flame such as with the use of more loudspeakers. With more loudspeakers, the focal amplitude will increase relative to the field amplitudes, thereby decreasing how loud it is away from the focus. In addition, the loudspeaker(s) could be installed in fixed locations and be able to focus and extinguish flames at many different locations in the same room without moving the loudspeakers (provided impulse responses at these different locations were already obtained), unlike the existing methods where the loudspeaker would need to be moved closer and pointed toward the flame.

More can be learned about how different frequencies and frequency ranges affect the TR peak amplitudes required to extinguish the flame. Perhaps using lower frequencies will decrease the peak amplitude threshold, as has been shown in other studies. In addition to this, work could be done to understand the size of flames that can be effectively extinguished using this method. The spatial extent of TR focusing is known to be approximately the size of the central wavelength of sound used in the band and thus larger flames may be more likely to be extinguished by using a lower frequency bandwidth, though nonlinear acoustic effects such as streaming are known to more likely occur with higher frequency content.

Data availability

The data will be made available upon request by contacting Brian E. Anderson.

Received: 27 June 2024; Accepted: 25 November 2024

Published online: 03 December 2024

References

- Xiong, C., Liu, Y., Xu, C. & Huang, X. Extinguishing the dripping flame by acoustic wave. *Fire Saf. J.* **120**, 103109 (2021).
- Friedman, A. N., Danis, P. I., Fiola, G. J., Barnes, C. A. & Stolarov, S. I. Acoustically enhanced water mist suppression of heptane fueled flames. *Fire Technol.* **54**, 1829–1840 (2018).

3. Xiong, C., Liu, Y., Xu, C. & Huang, X. Acoustical extinction of flame on moving firebrand for the fire protection in wildland-urban interface. *Fire Technol.* **57**, 1365–1380 (2021).
4. Taspinar, Y. S., Koklu, M. & Altin, M. Acoustic-driven airflow flame extinguishing system design and analysis of capabilities of low frequency in different fuels. *Fire Technol.* **58**, 1579–1597 (2022).
5. Friedman, A. N. & Stolarov, S. I. Acoustic extinction of laminar line-flames. *Fire Saf. J.* **93**, 102–113 (2017).
6. Xiong, C., Liu, Y., Fan, H., Huang, X. & Nakamura, Y. Fluctuation and extinction of laminar diffusion flame induced by external acoustic wave and source. *Sci. Rep.* **11**, 14402 (2021).
7. McKinney, D. & Dunn-Rankin, D. Acoustically driven extinction in a droplet stream flame. *Combust. Sci. Technol.* **161**, 27–48 (2000).
8. Xiong, C., Wang, Z. & Huang, X. Acoustic flame extinction by the sound wave or speaker-induced wind?. *Fire Saf. J.* **126**, 103479 (2021).
9. Zhang, Y.-J., Jamil, H., Wei, Y.-J. & Yang, Y.-J. Displacement and extinction of jet diffusion flame exposed to speaker-generated traveling sound waves. *Appl. Sci.* **12**, 12978 (2022).
10. Niegodajew, P. et al. Application of acoustic oscillations in quenching of gas burner flame. *Combust. Flame* **194**, 245–249 (2018).
11. DARPA. Instant flame suppression phase ii—final report. Tech. Rep., Defense Advanced Research Projects Agency (DARPA) (2012).
12. Beisner, E. et al. Acoustic flame suppression mechanics in a microgravity environment. *Microgravity Sci. Technol.* **27**, 141–144 (2015).
13. Ingård, U. & Labate, S. Acoustic circulation effects and the nonlinear impedance of orifices. *J. Acoust. Soc. Am.* **22**, 211–218. <https://doi.org/10.1121/1.1906591> (1950).
14. Boluriaan, S. & Morris, P. J. Acoustic streaming: from Rayleigh to today. *Int. J. Aeroacoust.* **2**, 255–292 (2003).
15. Raghavan, R. & Hrabovsky, G. Move me with your sound - acoustic streaming, its manifestations, and some of its uses. *Acoustics Today* **17**, 38–45 (2021).
16. Riley, N. *Acoustic Streaming*, chap. 30, 321–327 (Wiley, 1997).
17. Perelomova, A. & Wojda, P. Acoustic streaming caused by some types of aperiodic sound. buildup of acoustic streaming. *Arch. Acoust.* **34**, 625–639 (2009).
18. Oroscio, J. & Friend, J. Modeling fast acoustic streaming: Steady-state and transient flow solutions. *Phys. Rev. E* **106**, 045101. <https://doi.org/10.1103/PhysRevE.106.045101> (2022).
19. Garcia-Alcaide, V. et al. Numerical study of the aerodynamics of sound sources in a bass-reflex port. *Eng. Appl. Comput. Fluid Mech.* **11**, 210–224 (2017).
20. Roozen, N. B., Bockholts, M., van Eck, P. & Hirschberg, A. Vortex sound in bass-reflex ports of loudspeakers. part i. observation of response to harmonic excitation and remedial measures. *J. Acoust. Soc. Am.* **104**, 1914–1918 (1998).
21. Salvatti, A., Devantier, A. & Button, D. J. Maximizing performance from loudspeaker ports. *J. Audio Eng. Soc.* **50**, 19–45 (2002).
22. Devantier, A. & Rapoport, Z. Analysis and modeling of the bi-directional fluid flow in loudspeaker ports. In *Audio Engineering Society Convention 117* (2004).
23. Rossi, M., Esposito, E. & Tomasini, E. P. *PIV Application to Fluid Dynamics of Bass Reflex Ports* 259–270 (Springer, Berlin, 2008).
24. Xiong, C., Wang, Z. & Huang, X. Blow-off of diffusion flame by moving air vortex ring. *Exp. Thermal Fluid Sci.* **151**, 111059 (2024).
25. Bennewitz, J. W. et al. Periodic partial extinction in acoustically coupled fuel droplet combustion. *Combust. Flame* **189**, 46–61 (2018).
26. Wilk-Jakubowski, J. L. Analysis of flame suppression capabilities using low-frequency acoustic waves and frequency sweeping techniques. *Symmetry* **13**, 1299 (2021).
27. Stawczyk, P. & Wilk-Jakubowski, J. Non-invasive attempts to extinguish flames with the use of high-power acoustic extinguisher. *Open Eng.* **11**, 349–355 (2021).
28. Chen, L.-W., Wang, Q. & Zhang, Y. Flow characterisation of diffusion flame under non-resonant acoustic excitation. *Exp. Thermal Fluid Sci.* **45**, 227–233 (2013).
29. Zong, R., Kang, R., Liu, C., Zhang, Z. & Zhi, Y. Analysis of flame extinguishment and height in low frequency acoustically excited methane jet diffusion flame. *Microgravity Sci. Technol.* **30**, 237–242 (2018).
30. Huang, Y., Wang, M., Yang, K., Xu, C. & Wu, K. Role of acoustic wave on extinguishing flames coupling with water mist. *Case Stud. Therm. Eng.* **38**, 102367 (2022).
31. Niegodajew, P., Gruszka, K., Gnatowska, R. & Sofer, M. Application of acoustic oscillations in flame extinction in a presence of obstacle. *J. Phys. Conf. Ser.* **1101**, 012023. <https://doi.org/10.1088/1742-6596/1101/1/012023> (2018).
32. Allan, K. M., Kaminski, J. R., Bertrand, J. C., Head, J. & Sunderland, P. B. Laminar smoke points of wax candles. *Combust. Sci. Technol.* **181**, 800–811 (2009).
33. Parvulescu, A. & Clay, C. Reproducibility of signal transmissions in the ocean. *Radio Electron. Eng.* **29**, 223–228 (1965).
34. Fink, M. Time reversal in acoustics. *Contemp. Phys.* **37**, 95–109 (1996).
35. Anderson, B. E., Griffa, M., Johnson, P. A., Larmat, C. & Ulrich, T. J. Time reversal. *Acoustics Today* **4**, 5–15 (2008).
36. Anderson, B. E., Remillieux, M. C., Le Bas, P.-Y. & Ulrich, T. J. *Time Reversal Techniques*, chap. 14, 547–581 (Springer International Publishing, Cham, 2019).
37. Patchett, B. D. & Anderson, B. E. Nonlinear characteristics of high amplitude focusing using time reversal in a reverberation chamber. *J. Acoust. Soc. Am.* **151**, 3603–3614 (2022).
38. Willardson, M. L., Anderson, B. E., Young, S. M., Denison, M. H. & Patchett, B. D. Time reversal focusing of high amplitude sound in a reverberation chamber. *J. Acoust. Soc. Am.* **143**, 696–705 (2018).
39. Anderson, B. E. High amplitude time reversal focusing of sound and vibration. *Proc. Meetings Acoust.* **51**, 032001. <https://doi.org/10.1121/2.0001749> (2023).
40. Dos Santos, S. & Prevorsevsky, Z. Imaging of human tooth using ultrasound based chirp-coded nonlinear time reversal acoustics. *Ultrasonics* **51**, 667–674 (2011).
41. Tanter, M., Thomas, J.-L. & Fink, M. Focusing and steering through absorbing and aberrating layers: Application to ultrasonic propagation through the skull. *J. Acoust. Soc. Am.* **103**, 2403–2410 (1998).
42. Thomas, J.-L., Wu, F. & Fink, M. A. Time reversal focusing applied to lithotripsy. *Ultrason. Imaging* **18**, 106–121 (1996).
43. Thomas, J.-L. & Fink, M. A. Ultrasonic beam focusing through tissue inhomogeneities with a time reversal mirror: application to transskull therapy. *IEEE Trans. Ultrason. Ferroelectr. Freq. Control* **43**, 1122–1129 (1996).
44. Montaldo, G., Roux, P., Derode, A., Negreira, C. & Fink, M. Generation of very high pressure pulses with 1-bit time reversal in a solid waveguide. *J. Acoust. Soc. Am.* **110**, 2849–2857 (2001).
45. Le Bas, P.-Y., Ulrich, T. J., Anderson, B. E. & Esplin, J. J. A high amplitude, time reversal acoustic non-contact excitation (trance). *The Journal of the Acoustical Society of America* **134**, EL52–EL56 (2013).
46. Le Bas, P.-Y. et al. Damage imaging in a laminated composite plate using an air-coupled time reversal mirror. *Appl. Phys. Lett.* **107**, 184102. <https://doi.org/10.1063/1.4935210> (2015).
47. Farin, M., Prada, C. & de Rosny, J. Selective remote excitation of complex structures using time reversal in audible frequency range. *J. Acoust. Soc. Am.* **146**, 2510–2521 (2019).
48. Prada, C., Kerbrat, E., Cassereau, D. & Fink, M. Time reversal techniques in ultrasonic nondestructive testing of scattering media. *Inverse Prob.* **18**, 1761–1773. <https://doi.org/10.1088/0266-5611/18/6/320> (2002).

49. Young, S. M., Anderson, B. E., Hogg, S. M., Le Bas, P.-Y. & Remillieux, M. C. Nonlinearity from stress corrosion cracking as a function of chloride exposure time using the time reversed elastic nonlinearity diagnostic. *J. Acoust. Soc. Am.* **145**, 382–391 (2019).
50. Chakroun, N., Fink, M. & Wu, F. Time reversal processing in ultrasonic nondestructive testing. *IEEE Trans. Ultrason. Ferroelectr. Freq. Control* **42**, 1087–1098. <https://doi.org/10.1109/58.476552> (1995).
51. Young, S. M., Anderson, B. E., Willardson, M. L., Simpson, P. E. & Le Bas, P.-Y. A comparison of impulse response modification techniques for time reversal with application to crack detection. *J. Acoust. Soc. Am.* **145**, 3195–3207 (2019).
52. Wallace, C. B. & Anderson, B. E. High-amplitude time reversal focusing of airborne ultrasound to generate a focused nonlinear difference frequency. *J. Acoust. Soc. Am.* **150**, 1411–1423 (2021).
53. Patchett, B. D., Anderson, B. E. & Kingsley, A. D. Numerical modeling of Mach-stem formation in high-amplitude time-reversal focusing. *J. Acoust. Soc. Am.* **153**, 2724–2732 (2023).
54. Patchett, B. D., Anderson, B. E. & Kingsley, A. D. The impact of room location on time reversal focusing amplitudes. *J. Acoust. Soc. Am.* **150**, 1424–1433 (2021).
55. Yang, Y. et al. Self-navigated 3D acoustic tweezers in complex media based on time reversal. *Research* **2021**, 9781394. <https://doi.org/10.34133/2021/9781394> (2021). <https://doi.org/10.34133/2021/9781394>
56. Lewis, G. K. Jr. et al. Time-reversal techniques in ultrasound-assisted convection-enhanced drug delivery to the brain: Technology development and in vivo evaluation. *Proc. Meetings Acoust.* **11**, 020005. <https://doi.org/10.1121/1.3616358> (2011).
57. Tommiska, O. et al. FEM-based time-reversal technique for an ultrasonic cleaning application. *Appl. Acoust.* **193**, 108763 (2022).
58. Anderson, B. E., Clemens, M. & Willardson, M. L. The effect of transducer directivity on time reversal focusing. *J. Acoust. Soc. Am.* **142**, EL95–EL101 (2017).
59. Van Damme, B., Van Den Abele, K., Li, Y. & Matar, O. B. Time reversed acoustics techniques for elastic imaging in reverberant and nonreverberant media: An experimental study of the chaotic cavity transducer concept. *J. Appl. Phys.* **109** (2011).
60. Anderson, B. E., Ulrich, T. J. & Le Bas, P.-Y. Comparison and visualization of focusing wave fields from various time reversal techniques in elastic media. *J. Acoust. Soc. Am.* **134**, EL527–EL533 (2013).
61. Lessard, C. S. Window functions and spectral leakage. In *Signal Processing of Random Physiological Signals*, 175–193 (Springer, 2006).
62. Ribay, G., de Rosny, J. & Fink, M. A. Time reversal of noise sources in a reverberation room. *J. Acoust. Soc. Am.* **117**, 2866–2872 (2005).
63. Denison, M. H. & Anderson, B. E. Time reversal acoustics applied to rooms of various reverberation times. *J. Acoust. Soc. Am.* **144**, 3055–3066 (2018).
64. Kingsley, A. D. et al. Development of software for performing acoustic time reversal with multiple inputs and outputs. *Proc. Meetings Acoust.* **46**, 055003. <https://doi.org/10.1121/2.0001583> (2022).
65. OSHA (1983). (Occupational Safety and Health Administration). 29 CFR §1910.95 - Occupational noise exposure.
66. de Mello, P., Pérez, N., Adamowski, J. & Nishimoto, K. Wave focalization in a wave tank by using time reversal technique. *Ocean Eng.* **123**, 314–326 (2016).
67. Heaton, C., Anderson, B. E. & Young, S. M. Time reversal focusing of elastic waves in plates for an educational demonstration. *The Journal of the Acoustical Society of America* **141**, 1084–1092 (2017).
68. Barnes, L. A. et al. The physics of knocking over LEGO minifigures with time reversal focused vibrations for use in a museum exhibit. *J. Acoust. Soc. Am.* **151**, 738–751 (2022).
69. Williams, F. Progress in knowledge of flamelet structure and extinction. *Prog. Energy Combust. Sci.* **26**, 657–682 (2000).
70. Hu, L. A review of physics and correlations of pool fire behaviour in wind and future challenges. *Fire Saf. J.* **91**, 41–55 (2017).
71. Settles, G. S., Hackett, E. B., Miller, J. D. & Weinstein, L. M. Full-scale schlieren flow visualization. *Flow Visual.* **7**, 2–13 (1995).

Acknowledgements

The authors wish to thank Brigham Young University's College of Computational, Mathematical, and Physical Sciences for funding this research.

Author contributions

J.C. and B.A. conceived the experiment(s), J.C. conducted the experiment(s), J.C. and B.A. analyzed the results. All authors reviewed the manuscript.

Declarations

Competing interests

The authors declare no competing interests.

Additional information

Supplementary Information The online version contains supplementary material available at <https://doi.org/10.1038/s41598-024-81041-6>.

Correspondence and requests for materials should be addressed to B.E.A.

Reprints and permissions information is available at www.nature.com/reprints.

Publisher's note Springer Nature remains neutral with regard to jurisdictional claims in published maps and institutional affiliations.

Open Access This article is licensed under a Creative Commons Attribution-NonCommercial-NoDerivatives 4.0 International License, which permits any non-commercial use, sharing, distribution and reproduction in any medium or format, as long as you give appropriate credit to the original author(s) and the source, provide a link to the Creative Commons licence, and indicate if you modified the licensed material. You do not have permission under this licence to share adapted material derived from this article or parts of it. The images or other third party material in this article are included in the article's Creative Commons licence, unless indicated otherwise in a credit line to the material. If material is not included in the article's Creative Commons licence and your intended use is not permitted by statutory regulation or exceeds the permitted use, you will need to obtain permission directly from the copyright holder. To view a copy of this licence, visit <http://creativecommons.org/licenses/by-nc-nd/4.0/>.

© The Author(s) 2024